Supporting Information for
Short communication
Unraveling the drug distribution in brain enabled by MALDI MS imaging with laser-assisted chemical transfer

Shuai Guo, Kening Li, Yanwen Chen, Bin Li*

State Key Laboratory of Natural Medicines and School of Traditional Chinese Pharmacy, China Pharmaceutical University, Nanjing 210009, China

Received 22 August 2021; received in revised form 24 October 2021; accepted 3 November 2021

*Corresponding author. Tel./fax: +86 25 83271382
E-mail address: binli@cpu.edu.cn (Bin Li).

Materials and methods

Chemicals

The MALDI matrices of 2,5-dihydroxybenzoic acid (DHB), 1,5-diaminonapthalene (DAN), α-cyano-4-hydroxycinnamic acid (CHCA), 2,4,6-trihydroxy-acetophenone (THAP), and 2,6-dihydroxyacetophenone (DHAP) were purchased from Yuanye Biotechnology Co. Ltd (Shanghai, China). The drugs and regents of memantine, tacrine, xylazine, clonidine, lidocaine, lamotrigine, venlafaxine, imipramine, fluoxetine, olanzapine, clozapine, haloperidol, donepezil, quetiapine, risperidone (RSP), 9-hydroxy-risperidone (9-OH RSP), aripiprazole, 1,2-dipalmitoyl-sn-glycero-3-phosphocholine (PC(16:0/16:0)) and vanillin (98%) were obtained from Aladdin Chemistry Co. Ltd (Shanghai, China). Concentrated sulfuric acid, phosphoric acid (85%), chloroform, methanol, and acetonitrile were all HPLC grade and purchased from Merck (Darmstadt, Germany). Ultrapure deionized water was from a Milli-Q system (Millipore, Burlington, MA).

Animal dosing and tissue collection

Adult male ICR mice (6 weeks, 25–30 g) were purchased from Bikai Laboratory Animal Co. Ltd (Shanghai, China) and were housed in an air-conditioned, temperature-controlled room with the 14/10-hour light/dark cycle. Animal experiments were carried out following the Guidelines for Animal Experimentation of China Pharmaceutical University (Nanjing, China) and approved by the Animal Ethics Committee of this institution. All mice were intraperitoneally (i.p.) administered the central nervous system (CNS) drugs and euthanized by cervical dislocation 30 min after injection. The dosage and solvent system of these drugs were carefully determined based on our previous studies (Table S1). For the time-course study of RISP, brain samples were collected at 0.25, 0.5, 1, 2, 4, 8, 12, 24 h after a single dose of RISP (20 mg/kg) via i.p. injection. Following euthanasia, all the brains were rapidly dissected out, snap-frozen immediately in dry ice, and stored at storage at -80 °C for future use. Coronal, sagittal, and horizontal mouse brain sections were cut at 10 μm thickness on a cryostat at -20 °C (Leica CM3050, Germany) and thaw mounted onto conductive indium-tin-oxide (ITO) coated glass slides, respectively. All the tissue sections were dried for 10 min in a vacuum desiccator at room temperature prior to matrix coating.

Matrix application and characterization

Tissue sections mounted on ITO glass slides were coated with various matrices using a home-built electric field-assisted matrix coating system. A high voltage of 5 kV was applied to the conductive ITO slide to enhance the extraction of chargeable analytes from tissue to matrix layer as previously reported.[1] Matrices of DHB, CHCA, DAN, DHAP, and THAP were prepared at the concentration of 30 mg/mL in 80:20 acetonitrile: water. 190 μL of matrix solution were sprayed on tissue slides (0.42 mg/cm^2) at a flow rate of 4 mL/h. After matrix coating, solid-state

UV-vis spectra of ITO glass slides coated with different matrices were recorded using Hitachi U-3900 spectrophotometer (Tokyo, Japan).

LACT setup and process

As shown in Fig. 1A and Fig. S1, the laser-assisted chemical transfer (LACT) was carried out using a conventional used MALDI matrix as an intermediary layer to absorb laser photons and provide a mechanical push for chemical transfer. A diode laser source with the wavelength of 405 nm (LSR405SD, Lasever, China) was assembled on the LACT instrument. The laser power was precisely controlled by a set of neutral density filters (Union Optic, Wuhan, China) and pulse width modulation (PWM) based on Arduino Nano platform (Smart Projects, Italy). The real-time laser power illuminated on the sample surface was monitored by a laser power meter (VLP-2000, Ranbond Technology, Beijing, China). The laser beam was focused by an optical objective lens, and the distance between the exit of the lens and the target surface can be adjusted by an XYZ positioner to achieve the best focal length. The spot diameter of the focused laser was controlled to 150 μm and identified by the microscopical examination (Ts2r-FL, Nikon Corporation, Tokyo, Japan) of the width of the transferred stripe. A parameter, termed transfer threshold, is defined as the minimum real-time laser power necessary to achieve successful chemical transfer.

In the LACT process, the upper ITO slide coated with the tissue section and an energy absorption matrix layer was termed the donor slide. The laser beam was focused on the matrix layer from the backside of the donor slide to transfer a partial matrix-analyte mixture to another ITO slide referred as the acceptor slide. Introduce the laser from the backside of the acceptor slide could not propel material to the acceptor slide by the laser pulse. The donor slide was placed in close contact with the acceptor slide (gapless) and mounted on a 2D translation stage. The 2D stage moved at a constant speed of 3.5 mm s^{-1} in *x* dimension with 150 μm step size in *y* dimension. After transferring, no external force is needed to break two slides apart after the LACT experiment, and a well-defined pattern of chemical film was deposited on the acceptor slide. This film on the acceptor slide was eventually analyzed by matrix-assisted laser desorption/ionization (MALDI) mass spectrometry imaging (MSI). The morphology of transferred chemical film was observed by a stereomicroscope (Leica M165C, Leica Microsystems, Germany), and the thickness of this film was measured by a scanning electron microscope (SEM) (JS-3400N II, Hitachi, Ltd., Tokyo, Japan).

MALDI MSI and data analysis

All MALDI MS analysis was performed using an ultrafleXtreme MALDI TOF-TOF MS (Bruker Daltonics, U.S.) equipped with a Nd:YAG solid-state Smartbeam II laser (355 nm, 2 kHz). Data were acquired from *m/z* 100-1000 in positive ion reflection mode with 100 laser shots fired at 1 kHz. A laser step size of 200 μm with the “Ultra” footprint was set for the conventional MALDI

MSI and a step size of 50 μm with the “medium” footprint was set for high spatial resolution imaging. A mixture of drug standards of memantine, tacrine, imipramine, quetiapine, and aripiprazole were used to calibrate the instrument.

MALDI MS/MS was performed on both dosed tissue sections and drug standards to identify the detected CNS drugs, and the comparisons were also conducted between fragment ion peaks with the HMDB database to confirm their structures (https://hmdb.ca/spectra/ms_ms/search). The detailed information of detected analytes in this study is listed in Table S2.

To determine the limits of detection (LOD) (S/N=3) of CHCA-LACT and conventional MALDI method, the 0.5 μL aliquot from the dilution series of each drug standard was spotted on the cortex of the brain tissue section. To further investigate the quantitative ability of the proposed method, 0.5 μL of the standard solutions of venlafaxine at concentrations of 5, 10, 25, 50, 100, 250, and 500 ng μL^{-1} were spotted on the blank mouse brain section. For the tissue extinction coefficient (TEC) experiment, the standards of 16 CNS drugs were premixed with the CHCA solution at the final concentration of 100 μg/mL of each compound. The equal concentration mixture was then sprayed onto the glass slide containing the blank tissue sections. All samples were subsequently detected and imaged by MALDI MS, and the data were read and analyzed using flexAnalysis 3.4 and flexImaging 4.1 (Bruker Daltonics). The comparisons of peak intensities from different tissue regions were performed by extracting intensity data from defined regions of interest (ROI) by MSiReader v1.00. TEC values were calculated based on the relationship $TEC = I_{A,tissue}/I_{A,ref}$, where I_A is the averaged drug ion intensities on tissue and reference areas.[2] The color scale bar was located on the left side of the ion image, and its value represented the absolute intensities divided by 10. Statistical analyses were performed using OriginPro 2017 (OriginLab Corporation, Northampton, MA).

Detection of total lipids and proteins

To analyze the total amounts of lipids and proteins of tissue sections before and after CHCA-LACT treatment, the small pieces of glass coated with the tissue were removed from the standard ITO slide by glass cutter and were immersed in the 1.5 mL chloroform/methanol (1:2, *v/v*) solution. After a 1 min vortex oscillation and 30 min ultrasonic extraction, the extracted solvent was collected and centrifuged at 13,000×g for 15 min at 4°C. For lipid measurement, the supernatant was transferred into a glass vial and dried at 90°C to evaporate the chloroform and methanol. Then, 100 μL of 98% sulfuric acid was added, and the solution was incubated for 20 minutes at 90°C. A microplate reader (SpectraMax M5, Molecular Devices, USA) was used to measure background absorbance. A volume of 50 μL vanillin-phosphoric acid reagent was added to each well for color development. After cooling down to room temperature for 10 minutes, absorbance was measured at 540 nm as previously reported[3]. For protein measurement, the protein precipitation of tissues was collected for evaporation of the solvent

at 90°C. Then, the extracted protein was dissociated in 1% SDS (20 μL) and measured by the BCA assay kit (Shanghai Yuanye Biotechnology, Shanghai, China).[4]

Sample preparation and LC-MS/MS analysis

To confirm the results of the time-course study of RSP based CHCA-LACT MALDI imaging, both RSP and 9-OHRSP were extracted from the tissues of varying specific brain regions and time points as previously reported[5]. Briefly, thick tissue sections (1 mm) adjacent to the sections used for MALDI MSI were acquired and dissected with a tissue punch (1 mm i.d.) at regions of the frontal cortex, striatum, midbrain, hippocampal, and cerebellum after 0.5 h of administration and at stratum region after 0.25, 0.5, 1, 2, 4, 8, 12 and 24 h of administration. Then, the tissue punch samples were accurately weighed and homogenized in cold normal saline (1:10, W/V) by a vortex agitator and ultrasonic bath for 30 min. 20 μL of each homogenate was mixed with 200 μL acetonitrile containing 100 ng/mL internal standard (IS), vortexed for 5 min, and centrifuged at 13,000×g for 10 min at 4°C. 2 μL of each respective supernatant was injected into the LC-MS/MS system for drug content analysis.

LC-MS/MS experiments were performed using an Agilent 6460 QQQ mass spectrometer connected to an Agilent 1260 series UHPLC system (Agilent Technologies, CA, USA) based on our previous report[5]. In detail, analytes were separated with an Agilent XDB C18 column (4.6 mm × 50 mm, 1.8 μm) preceded by a guard column (5 mm × 4.6 mm, 1.8 μm, Agilent Eclipse XDB-C18) at 30 ºC. Mobile phase A and B were water containing 0.1% formic acid (*v/v*) and methanol, respectively. The flow rate of the mobile phase was 0.4 mL/min, and the gradient program was conducted as follows: 0-3 min, 5%-35% B; 3-5 min, 35% B; 6-9 min, 35%-65% B; 9-10 min, 65%-95% B; and 10-11 min, 95% B. The injection volume was 2 μL, and the mass spectrometer was operated in positive ion mode and the ESI source parameters were as follows: drying gas temperature, 350 °C; drying gas flow, 10.0 L/min; sheath gas temperature, 300 °C; sheath gas flow, 11 L/min; nebulizer pressure, 45 psi; capillary voltage, 3.5 kV. Quantification analysis was performed in multiple-reaction monitoring (MRM) mode with the ion transitions of *m/z* 441 to 191 for RSP, *m/z* 427 to 207 for 9-OHRSP, *m/z* 384 to 253 for IS, respectively. The collision energy was set to 45 eV for all the endogenous metabolites. Data collection and processing were conducted with MassHunter Workstation 5.0 (Agilent Technologies, USA).

Fluorescence microscopy

Fluorescence imaging was performed on the tissue section from fluorescein sodium salt dosed mouse brain (100 mg/kg) at 0.5 h after administration. Fluorescein has an excitation maximum of 490 nm and an emission maximum of 518 nm. Fluorescence images were acquired using a fluorescent microscope (Ts2r-FL, Nikon Corporation, Tokyo, Japan) with 0.6 s exposure time.

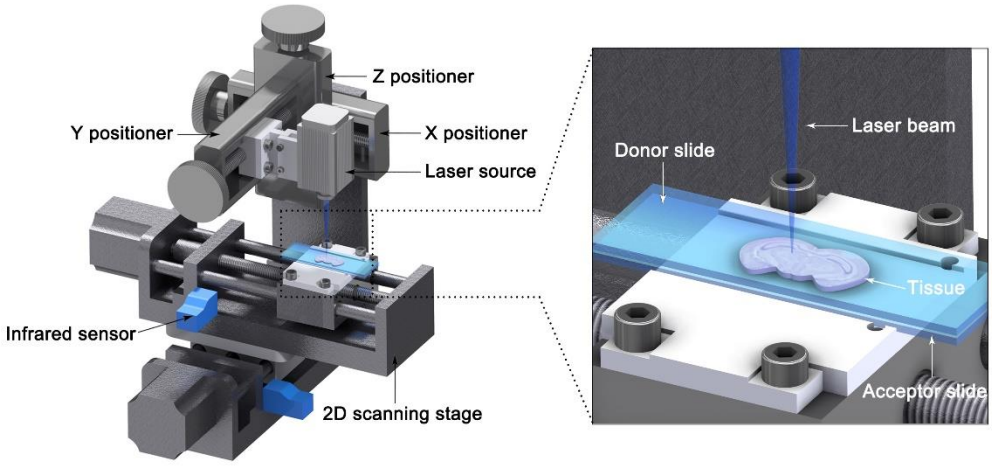

Figure S1 Schematic experimental setup of LACT system.

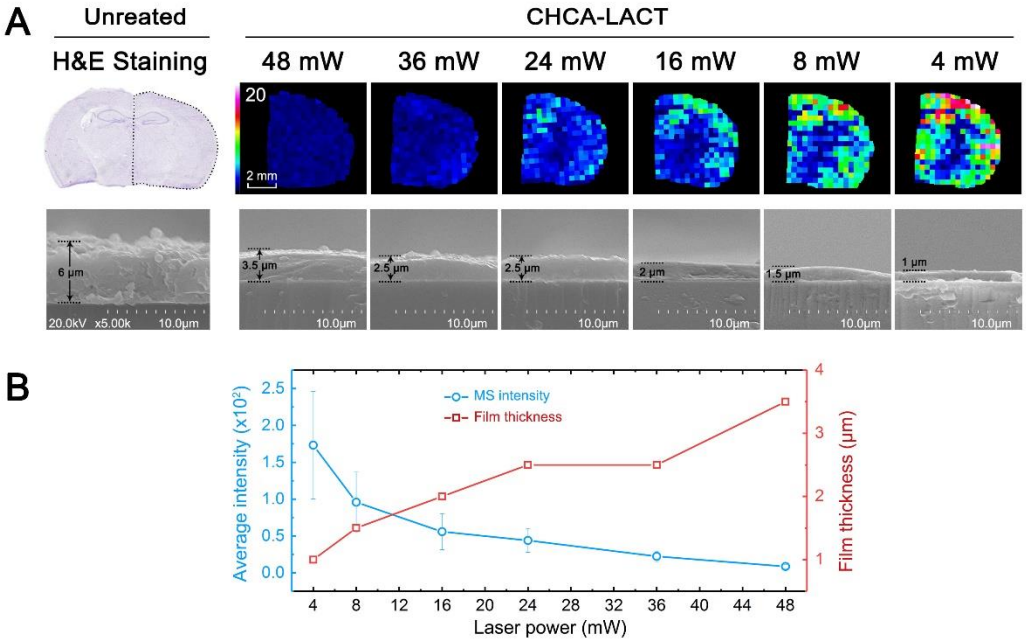

Figure S2 The influence of the thickness of transferred film on signal intensities of exogenous drug venlafaxine. (A) Ion images of venlafaxine and SEM photos of transferred chemical films obtained by the CHCA-LACT method at different laser powers. SEM images were acquired from the fracture surface of acceptor slides coated with transferred films. (B) Dependence of thickness and average signal intensities of transferred chemical films acquired by CHCA-LACT at different laser powers. Error bars indicate the standard deviations of 200 mass spectra acquired from the whole ion images.

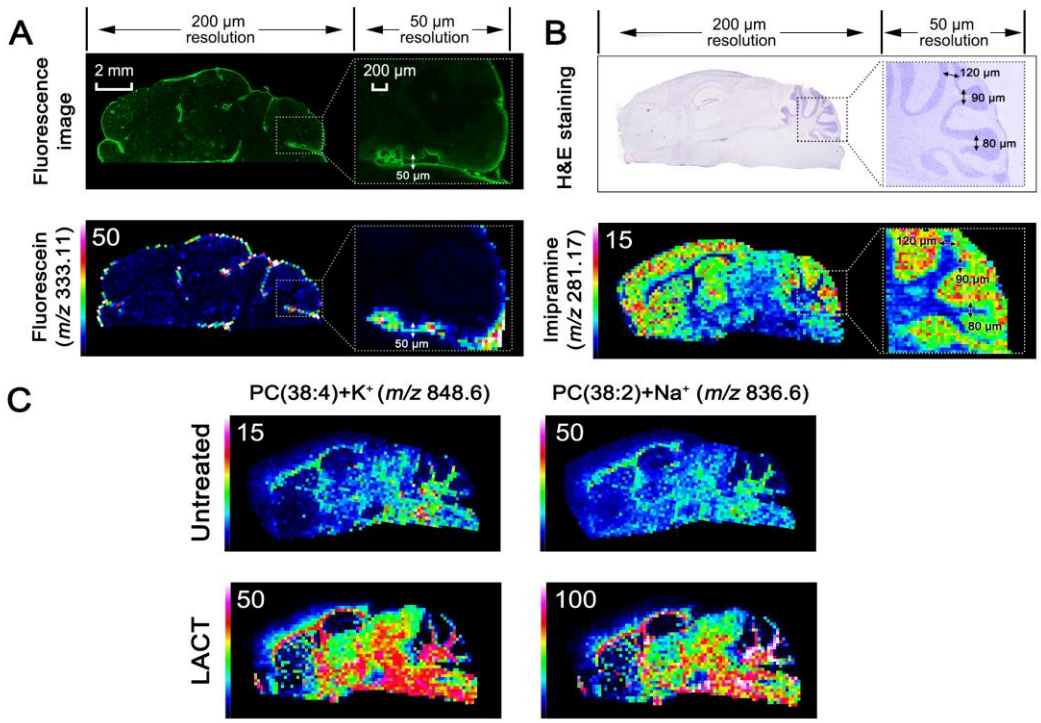

Figure S3 Evaluation of possible compound delocalization occurred in LACT by using fluorescent, H&E and MALDI MS imaging. (A) Fluorescence image of mouse brain section dosed with fluorescein and corresponding ion image (*m/z* 333.11) obtained from CHCA-LACT MALDI MSI at 200 μm and 50 μm step size, respectively. (B) H&E-stained image of brain section dosed with imipramine and corresponding ion image (*m/z* 281.17) obtained from CHCA-LACT MALDI MSI at 200 μm and 50 μm step size, respectively. (C) Ion images of two lipids obtained from dosed brain sections treated with and without LACT by using MALDI MSI at 200 μm step size, respectively.

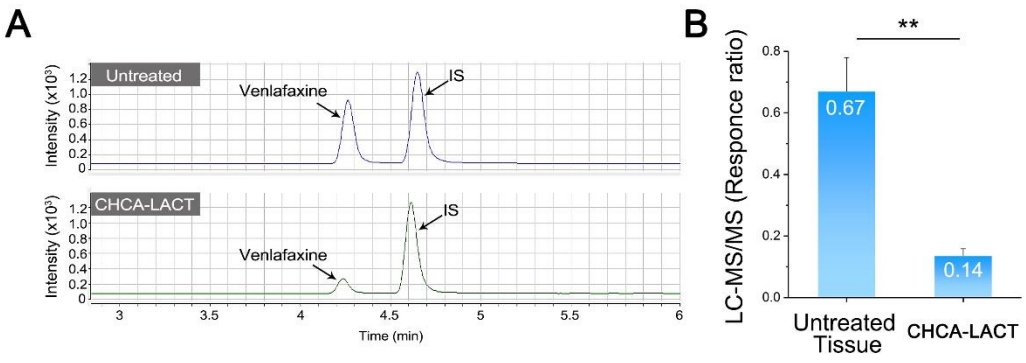

Figure S4 The relative amount of venlafaxine determined in tissue sections before and after LACT treatment. (A) LC-MS/MS chromatogram and (B) relative levels of venlafaxine in tissue sections before and after LACT treatment.

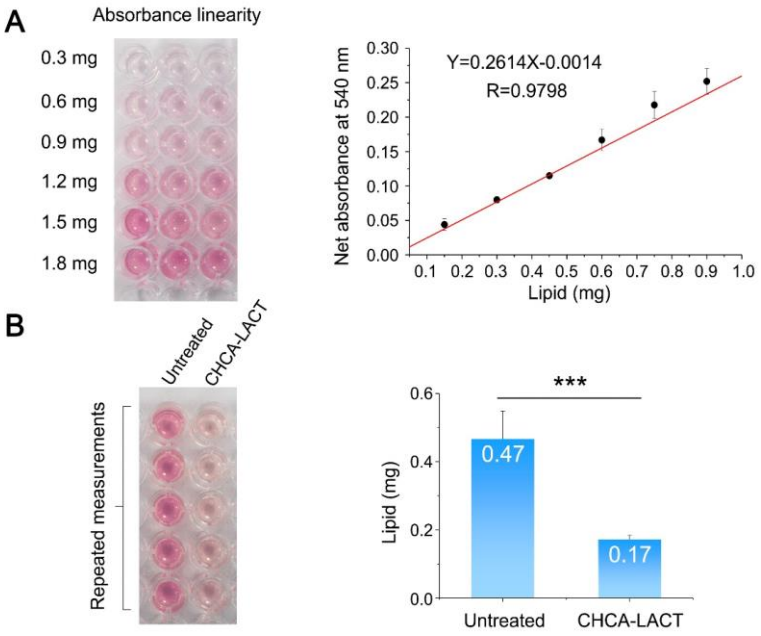

Figure S5 Detection of total lipids from untreated tissue sections and transferred films produced by CHCA-LACT. (A) Absorbance linearity of lipid standard of PC(16:0/16:0). Data points represent the mean of three replicate samples. (B) Total amounts of lipids from untreated tissue sections and transferred films produced by CHCA-LACT. Error bars indicate the deviation of five independent experiments.

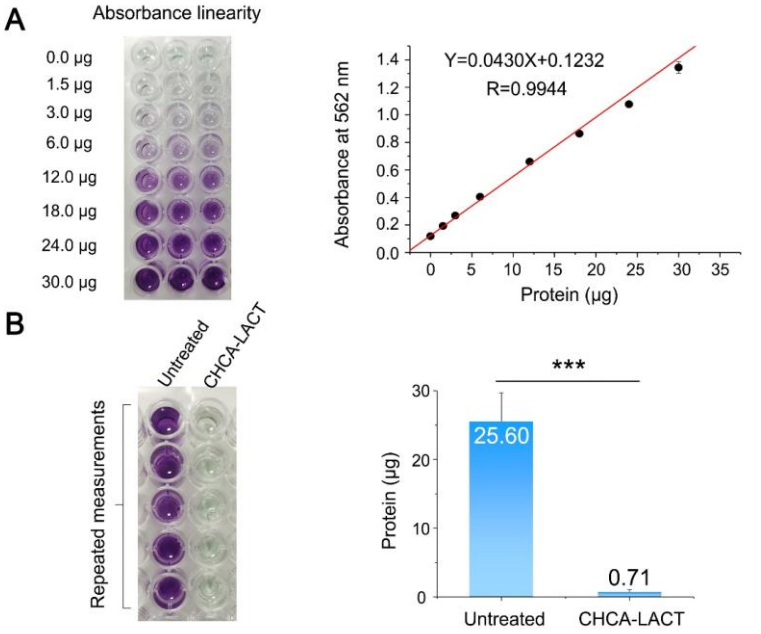

Figure S6 Detection of total proteins from untreated tissue sections and transferred films produced by CHCA-LACT. (A) Absorbance linearity of protein standard of bovine serum albumin. Data points represent the mean of three replicate samples. (B) Total amounts of protein from untreated tissue sections and transferred films produced by CHCA-LACT. Error bars indicate the deviation of five independent experiments.

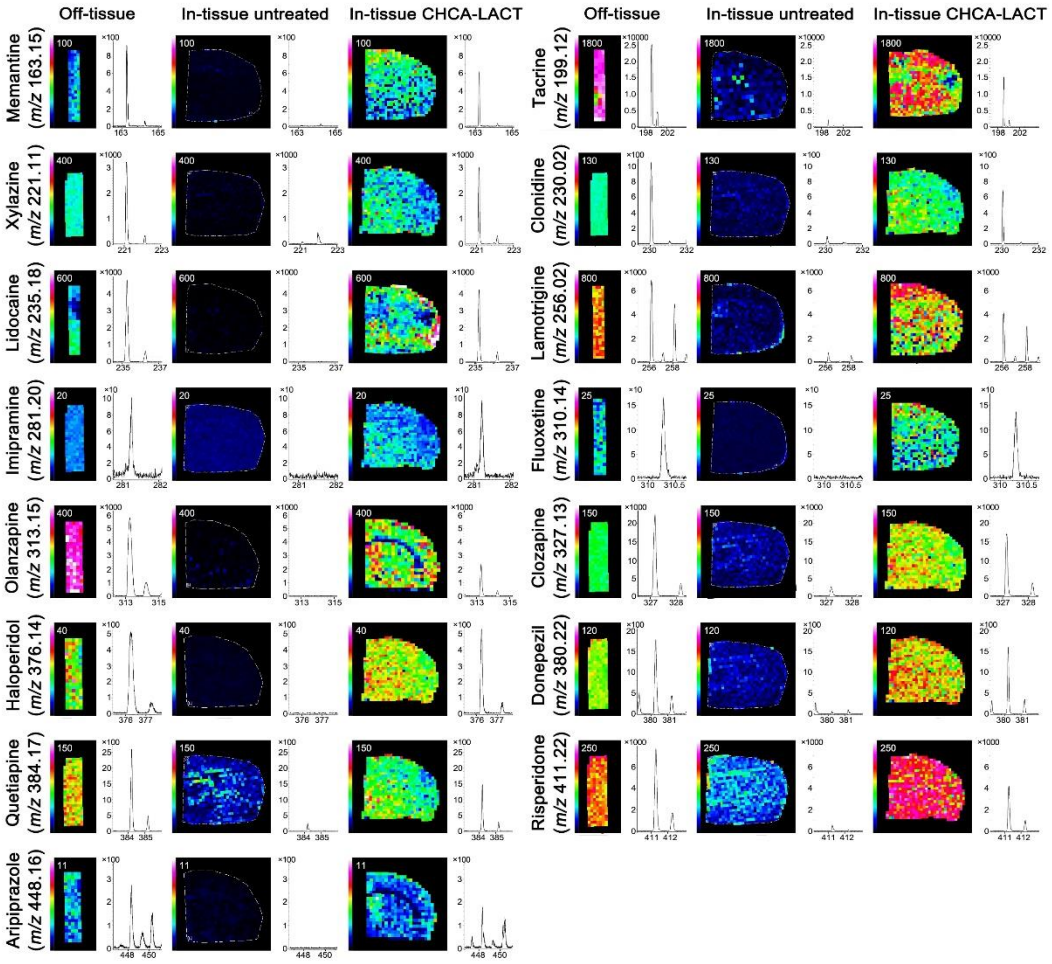

Figure S7 Comparison of the ion suppression effects of 15 CNS drugs in tissue sections with and without CHCA-LACT treatment. Ion images and representative mass spectra of 15 CNS drugs were acquired in the off-tissue glass region, in-tissue region of untreated tissue, and in-tissue region of the transferred film generated by CHCA-LACT, respectively.

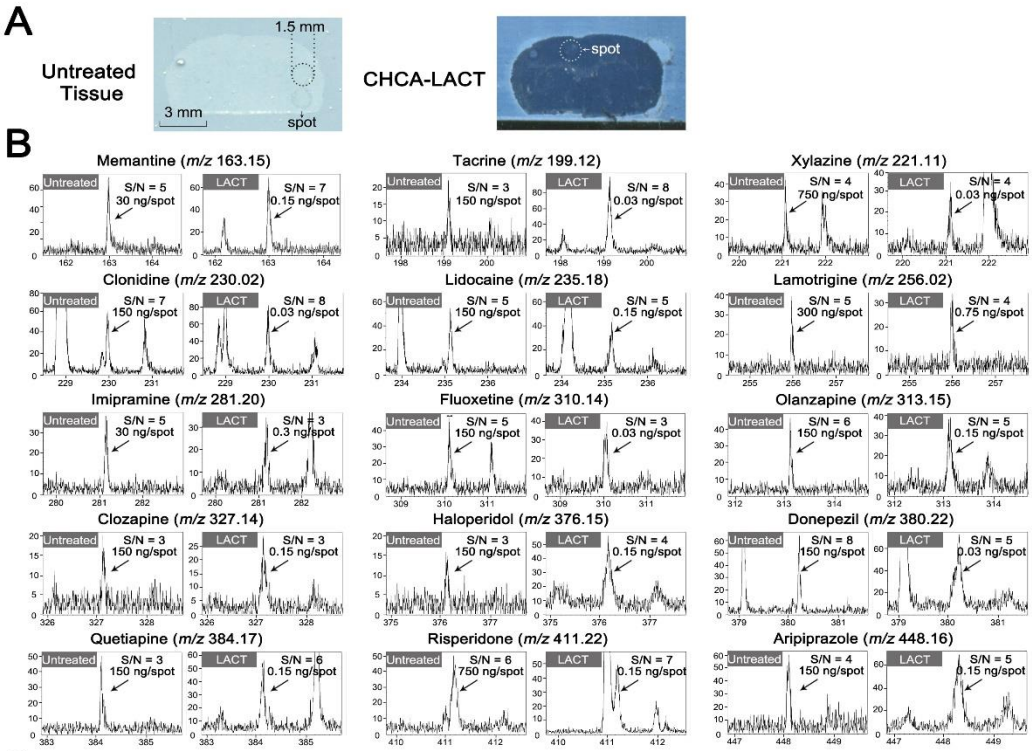

C

Drugs	Memantine	Tacrine	Xylazine	Clonidine	Lidocaine	Lamotrigine	Venlafaxine	Imipramine
Untreated LOD (ng/spot)	30	150	750	150	150	300	150	30
CHCA-LACT LOD (ng/spot)	0.15	0.03	0.03	0.03	0.15	0.75	0.15	0.3

Drugs	Fluoxetine	Olanzapine	Clozapine	Haloperidol	Donepezil	Quetiapine	Risperidone	Aripiprazole
Untreated LOD (ng/spot)	150	150	150	150	150	150	750	150
CHCA-LACT LOD (ng/spot)	0.03	0.15	0.15	0.15	0.03	0.15	0.15	0.15

Figure S8 Comparison of the LODs of CNS drugs in tissue sections with and without CHCA-LACT treatment. (A) Optical photo of the tissue section spotted with the drug standard before and after the CHCA-LACT treatment. (B) Representative mass spectra of 15 CNS drugs acquired in tissue sections with and without CHCA-LACT treatment at the LOD level. (C) Numerical values of the LODs for all 16 CNS drugs of the above two treatments.

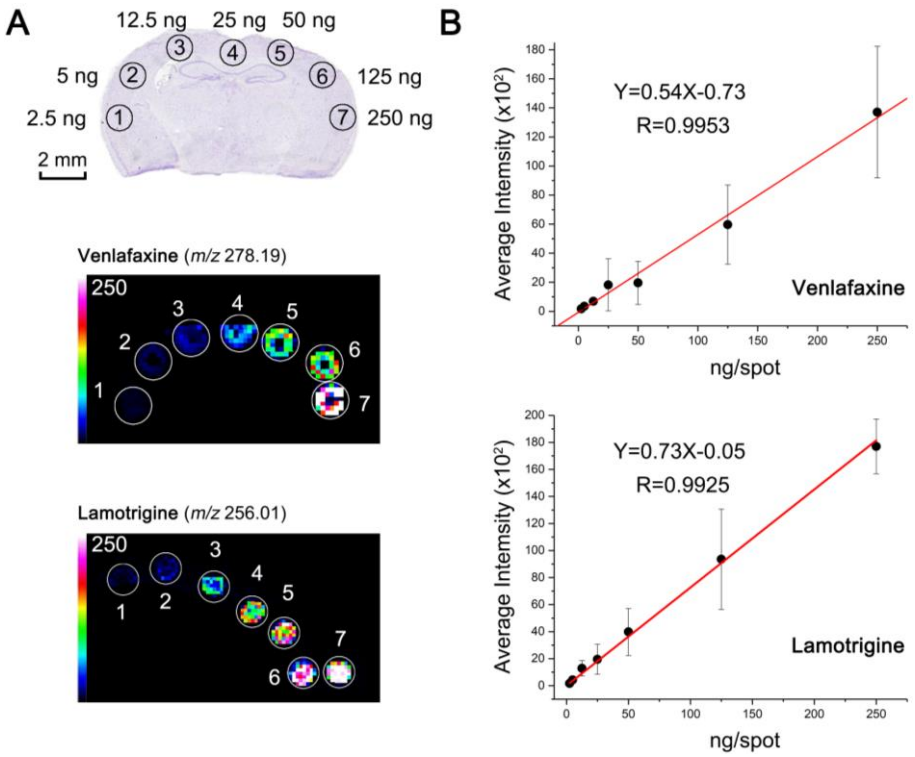

Figure S9 The linearity of venlafaxine and lamotrigine in coronal brain section obtained by MALDI MSI with LACT. The serial dilutions of drug standard were manually spotted (0.5 μL) on the cortex of the blank brain tissue section, which was subsequently transferred by LACT and analyzed by MALDI MSI. Error bars indicate the standard deviations of 20 mass spectra acquired from the ROI regions.

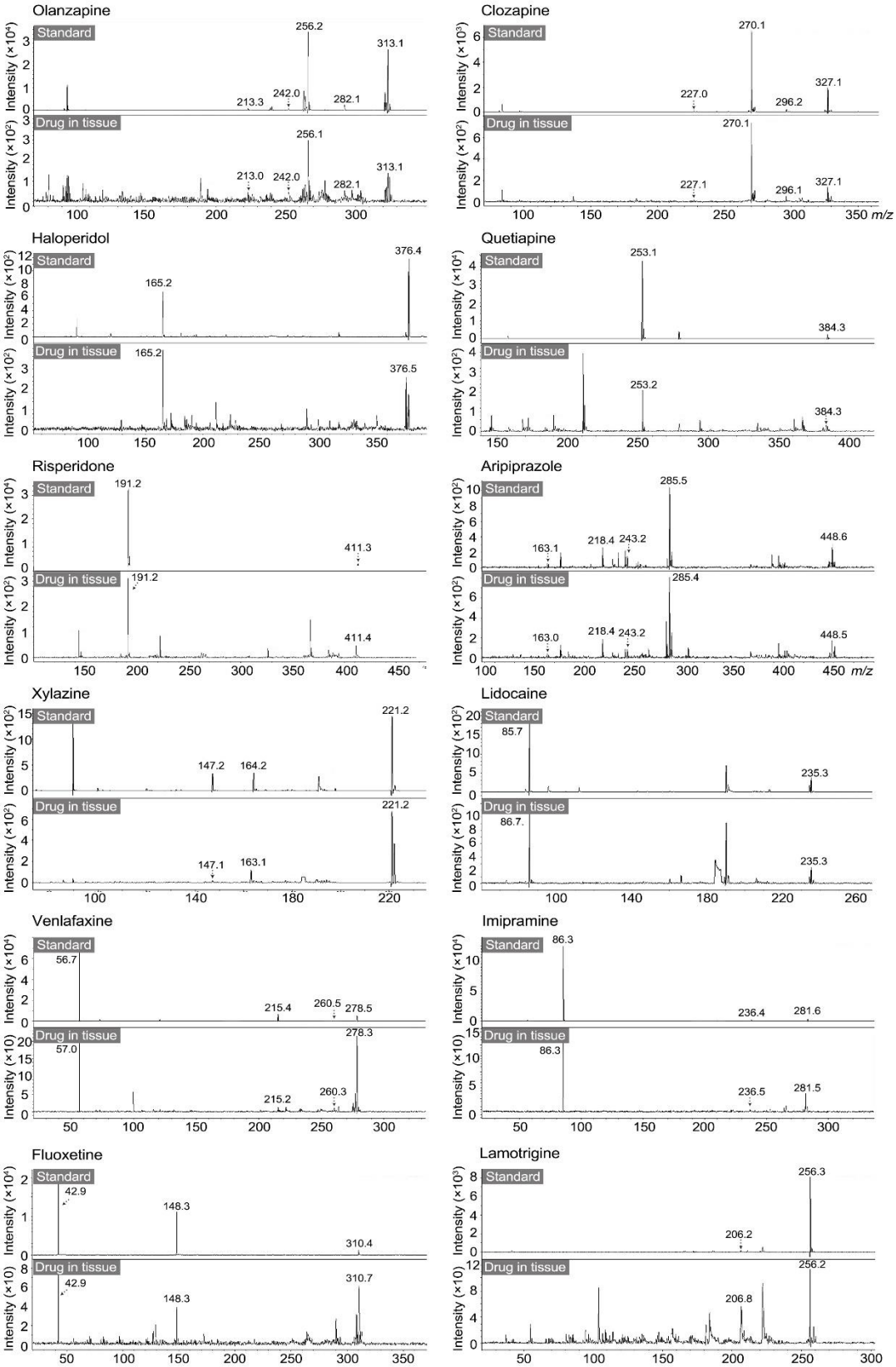
Olanzapine
Standard
Drug in tissue
Clozapine
Standard
Drug in tissue
Haloperidol
Standard
Drug in tissue
Quetiapine
Standard
Drug in tissue
Risperidone
Standard
Drug in tissue
Aripiprazole
Standard
Drug in tissue
Xylazine
Standard
Drug in tissue
Lidocaine
Standard
Drug in tissue
Venlafaxine
Standard
Drug in tissue
Imipramine
Standard
Drug in tissue
Fluoxetine
Standard
Drug in tissue
Lamotrigine
Standard
Drug in tissue
m/z

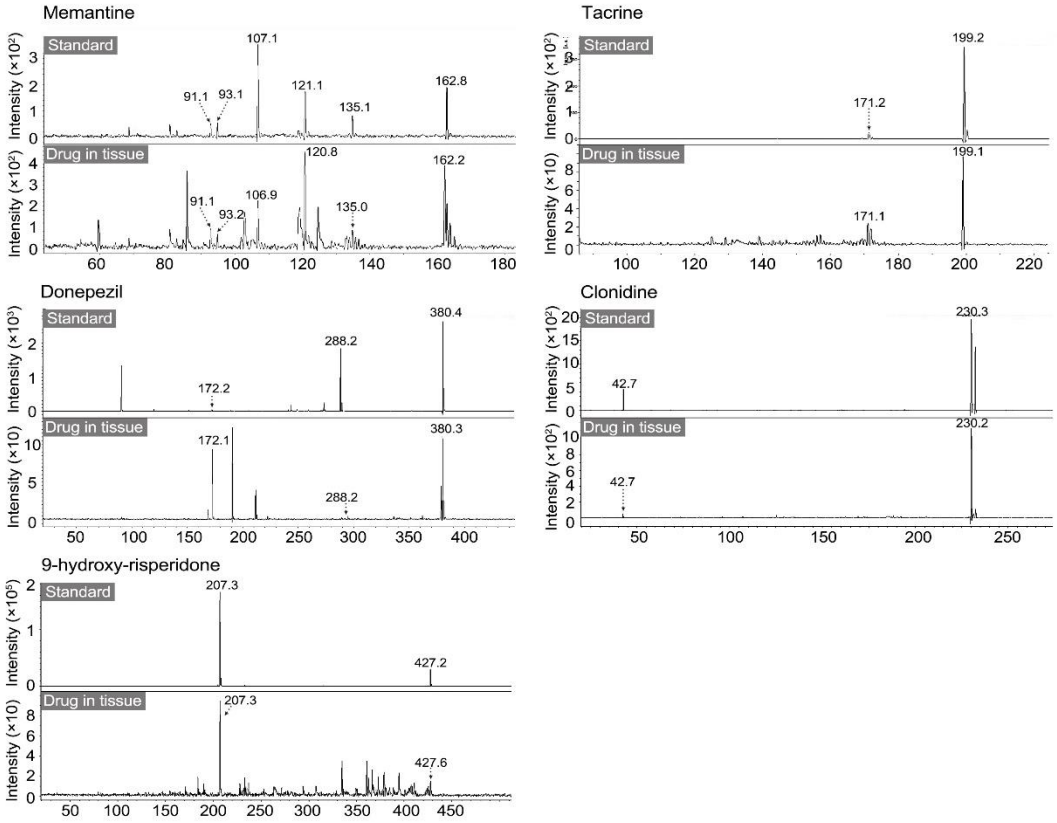

Figure S10 Tandem mass spectra of CNS drug standards and dosed brain tissue sections treated with CHCA-LACT. The detected fragments were further compared with the theoretical MS/MS pattern derived from the HMDB database (**Table S2**).

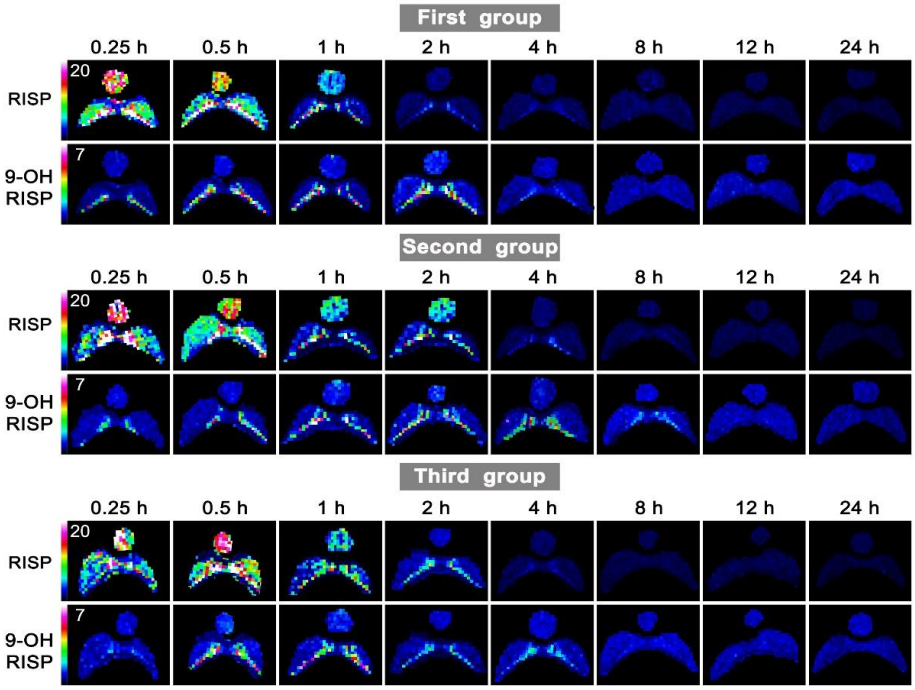

Figure S11 Repeated measurements of RISP and 9-OH RSP using CHCA-LACT on three groups of tissue samples acquired at various time points.

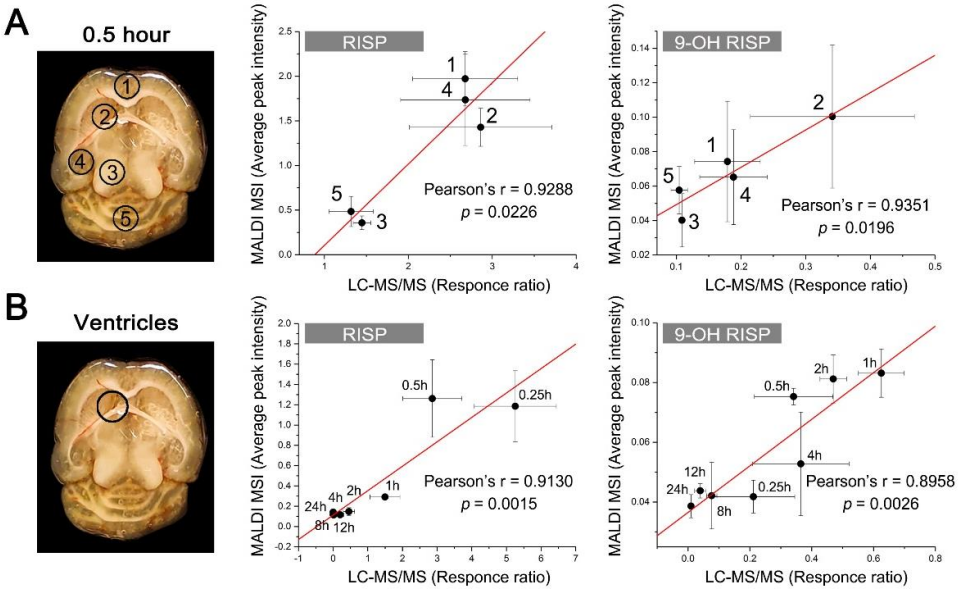

Figure S12 Correlation of CHCA-LACT MALDI MSI and LC-MS/MS methods for analyzing RISP and 9-OH RSP in various brain regions at different time points. (A) Correlation of CHCA-LACT MALDI MSI and LC-MS/MS for detecting RISP and 9-OH RSP in various brain regions at 0.5 h after administration. 1 frontal cortex, 2 ventricles, 3 midbrains, 4 hippocampi, 5 cerebella. (B) Correlation of the above two methods for detecting RISP and 9-OH RSP in the ventricular region at different time points. Error bars indicate the deviation of three independent experiments.

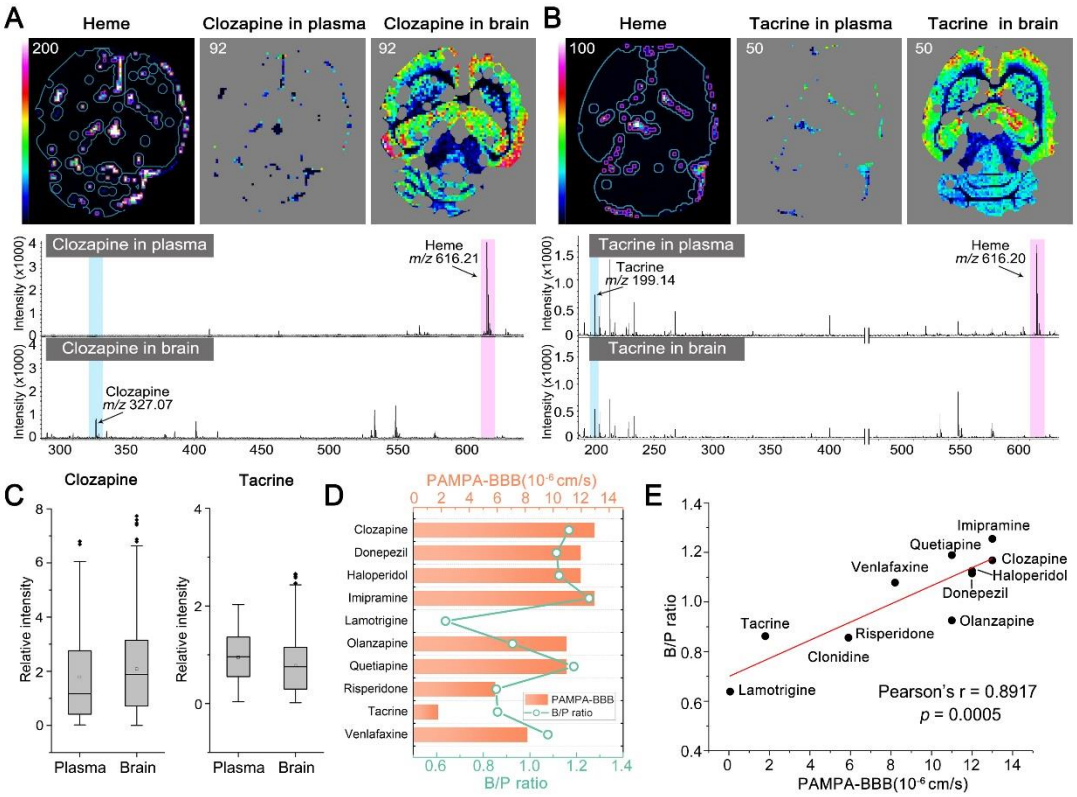

Figure S13 Screening brain penetration of different CNS drugs with CHCA-LACT MALDI MSI method. (A and B) Ion images and representative mass spectra of clozapine and tacrine in brain parenchyma region (blue line) and plasma (purple line) region of the mouse brain. (C) Calculated average intensities of clozapine and tacrine in the brain parenchyma and plasma regions. (D) Assessing brain penetrations of 10 CNS drugs with the B/P ratios acquired from MSI data and PAMPA-BBB data in previous studies. (E) Correlation of brain penetration between PAMPA-BBB and B/P ratio.

Table S1 The dosage and solvent system for the CNS drugs used in this study

No.	Drugs	Solvent System	Dosage	Reference
1	Memantine	Normal saline	25 mg/kg	[6]
2	Tacrine	Normal saline	10 mg/kg	[7]
3	Xylazine	Normal saline	10 mg/kg	[8]
4	Clonidine	Normal saline	30 mg/kg	[9]
5	Lidocaine	10% DMSO in normal saline	30 mg/kg	[10]
6	Lamotrigine	10% DMSO in normal saline	25 mg/kg	[11]
7	Venlafaxine	Normal saline	20 mg/kg	[12]
8	Imipramine	Normal saline	30 mg/kg	[13]
9	Fluoxetine	10% DMSO in normal saline	30 mg/kg	[14]
10	Olanzapine	10% DMSO in normal saline	10 mg/kg	[15]
11	Clozapine	10% DMSO in 10% β-cyclodextrin	10 mg/kg	[16]
12	Haloperidol	10% DMSO in normal saline	20 mg/kg	[17]
13	Donepezil	Normal saline	10 mg/kg	[18]
14	Quetiapine	10% DMSO in normal saline	10 mg/kg	[19]
15	Risperidone	10% DMSO in normal saline	10 mg/kg	[20]
16	Aripiprazole	10% DMSO in 10% β-cyclodextrin	20 mg/kg	[21]

Table S2 Analytes detected in mouse brain based on CHCA-LACT MALDI MS.

No.	Molecular Formula	Compunds	Observed *m/z*	Theoretical *m/z*	Ion Form	Observed MS/MS Fragments	Theoretical MS/MS Fragments
1	C12H21N	Memantine	163.16	163.1481	[M-NH3+H]+	91.1/93.2/106.9 /120.8/135.0/162.2	91.1/93.2/107.1 /121.1/135.1/162.8
2	C13H14N2	Tacrine	199.14	199.1230	[M+H]+	171.1/199.1	171.1/199.1
3	C12H16N2S	Xylazine	221.07	221.1107	[M+H]+	147.1/163.1/221.2	147.1/163.1/221.2
4	C9H9Cl2N3	Clonidine	229.97	230.0246	[M+H]+	42.7/230.2	42.0/230.0
5	C14H22N2O	Lidocaine	235.18	235.1805	[M+H]+	86.1/235.3	85.7/235.2
6	C9H7Cl2N5	Lamotrigine	256.01	256.0151	[M+H]+	206.8/256.2	206.0/256.0
7	C17H27NO2	Venlafaxine	278.19	278.2115	[M+H]+	57.0/215.2/260.3 /278.3	57.1/215.1/260.1 /278.2
8	C19H24N2	Imipramine	281.17	281.2012	[M+H]+	86.3/236.5/281.5	86.1/236.1/281.2
9	C17H18F3NO	Fluoxetine	310.11	310.1413	[M+H]+	42.9/148.3/310.7	44.0/148.1/310.1
10	C17H20N4S	Olanzapine	313.08	313.1481	[M+H]+	213.0/242.0/256.1 /282.1/313.1	213.0/242.1/256.1 /282.1/313.1
11	C18H19ClN4	Clozapine	327.08	327.1371	[M+H]+	227.1/270.1/296.1 /327.1	227.0/270.1/296.1 /327.1
12	C21H23ClFNO2	Haloperidol	376.05	376.1474	[M+H]+	165.2/376.5	165.1/376.1
13	C24H29NO3	Donepezil	380.09	380.2220	[M+H]+	172.1/288.2/380.3	172.1/288.2/380.2
14	C21H25N3O2S	Quetiapine	384.05	384.1740	[M+H]+	253.1/384.3	253.0/384.2
15	C23H27FN4O2	Risperidone	411.07	411.2191	[M+H]+	191.2/411.4	191.1/411.2
16	C23H27Cl2N3O 2	Aripiprazole	448.26	448.1553	[M+H]+	163.0/218.4/243.2 /285.4/448.5	164.0/218.1/243.0 /285.1/448.2
17	C23H27FN4O3	9-hydroxy-risperidone	427.06	427.2140	[M+H]+	207.3/427.6	207.1/427.2
18	C20H12O5	Fluorescein	333.11	333.0758	[M+H]+		
19	C34H32FeN4O4	Heme b	616.17	616.1768	[M]+		

References

1. Guo S, Wang Y, Zhou D, Li Z. Electric field-assisted matrix coating method enhances the detection of small molecule metabolites for mass spectrometry imaging. *Anal Chem*. 2015;87(12):5860-5.
2. Taylor AJ, Dexter A, Bunch J. Exploring Ion Suppression in Mass Spectrometry Imaging of a Heterogeneous Tissue. *Anal Chem*. 2018;90(9):5637-45.
3. Cheng YS, Zheng Y, VanderGheynst JS. Rapid quantitative analysis of lipids using a colorimetric method in a microplate format. *Lipids*. 2011;46(1):95-103.
4. Olson BJ, Markwell J. Assays for determination of protein concentration. *Curr Protoc Protein Sci*. 2007;48(1):3.4. 1-3.4. 29.
5. Chen Y, Tang W, Gordon A, Li B. Development of an Integrated Tissue Pretreatment Protocol for Enhanced MALDI MS Imaging of Drug Distribution in the Brain. *J Am Soc Mass Spectrom*. 2020.
6. Notartomaso S, Scarselli P, Mascio G, Liberatore F, Mazzon E, Mammana S, et al. N-Acetylcysteine causes analgesia in a mouse model of painful diabetic neuropathy. *Mol Pain*. 2020;16.
7. Vallianatou T, Shariatgorji M, Nilsson A, Fridjonsdottir E, Kallback P, Schintu N, et al. Molecular imaging identifies age-related attenuation of acetylcholine in retrosplenial cortex in response to acetylcholinesterase inhibition. *Neuropsychopharmacology*. 2019;44(12):2091-8.
8. Gergye CH, Zhao Y, Moore RH, Lee VK. A Comparison of Ketamine or Etomidate Combined with Xylazine for Intraperitoneal Anesthesia in Four Mouse Strains. *J Am Assoc Lab Anim Sci*. 2020;59(5):519-30.
9. Ushijima I, Katsuragi T, Furukawa T. Involvement of adenosine receptor activities in aggressive responses produced by clonidine in mice. *Psychopharmacology*. 1984;83(4):335-9.
10. Bittencourt AL, Takahashi RN. Mazindol and lidocaine are antinociceptives in the mouse formalin model: involvement of dopamine receptor. *Eur J Pharmacol*. 1997;330(2-3):109-13.
11. Izadpanah F, Arab F, Zarghami A, Bijani A, Kazemi S, Moghadamnia AA. The effect of lamotrigine on learning in mice using the passive avoidance model. *Epilepsy Behav*. 2017;69:1-6.
12. Bukhari IA, Dar A. Behavioral profile of Hypericum perforatum (St. John's Wort) extract. A comparison with standard antidepressants in animal models of depression. *Eur Rev Med Pharmacol Sci*. 2013;17(8):1082-9.
13. Podolan M, Dos Santos J, Walber T, Possamai F, Viola GG, Lino de Oliveira C. A single injection of imipramine affected proliferation in the hippocampus of adult Swiss mice depending on the route of administration, doses, survival time and lodging conditions. *J Chem Neuroanat*. 2019;100:101655.
14. Hemmati S, Sadeghi MA, Jafari RM, Yousefi-Manesh H, Dehpour AR. The antidepressant effects of GM-CSF are mediated by the reduction of TLR4/NF-?B-induced IDO expression. *J Neuroinflammation*. 2019;16.
15. Pinna A, Costa G, Contu L, Morelli M. Fos expression induced by olanzapine and risperidone in the central extended amygdala. *Eur J Pharmacol*. 2019;865.

16. Li CH, Stratford RE, Jr., Velez de Mendizabal N, Cremers TI, Pollock BG, Mulsant BH, et al. Prediction of brain clozapine and norclozapine concentrations in humans from a scaled pharmacokinetic model for rat brain and plasma pharmacokinetics. *J Transl Med*. 2014;12:203.
17. Gianutsos G, Drawbaugh RB, Hynes MD, Lal H. Behavioral evidence for dopaminergic supersensitivity after chronic haloperidol. *Life Sci*. 1974;14(5):887-98.
18. Wong JC, Thelin JT, Escayg A. Donepezil increases resistance to induced seizures in a mouse model of Dravet syndrome. *Ann Clin Transl Neurol*. 2019;6(8):1566-71.
19. Yan B, Bi X, He J, Zhang Y, Thakur S, Xu H, et al. Quetiapine attenuates spatial memory impairment and hippocampal neurodegeneration induced by bilateral common carotid artery occlusion in mice. *Life Sci*. 2007;81(5):353-61.
20. Yulug B, Yildiz A, Güzel O, Kilic E, Schäbitz WR, Kilic E. Risperidone attenuates brain damage after focal cerebral ischemia in vivo. *Brain Res Bull*. 2006;69(6):656-9.
21. Saraei M, Samadzadeh N, Khoeini J, Shahnazi M, Nassiri-Asl M, Jahanihashemi H. In vivo anti-Toxoplasma activity of aripiprazole. *Iran J Basic Med Sci*. 2015;18(9):938-41.